A new approximation method for scattering by large arrays

I. Thompson[†*], **C. M. Linton**[†] **and R. Porter**[‡]

[†]Dept. of Mathematical Sciences, Loughborough University, Loughborough, Leics. LE11 3TU, UK

[‡] Dept. of Mathematics, University of Bristol, Bristol BS8 1TW, UK

*Email: i.thompson@lboro.ac.uk

1 Introduction

The interaction of water waves with large arrays of bodies is of considerable importance in the design of many offshore structures. A standard technique based on separation of variables can be used to model such situations [1], however this is devised for arbitrary configurations of scatterers. When the number of bodies is large, expensive numerical computations are required, and understanding of the interaction effects is easily lost. In this article, we will develop a new method which aims to exploit the simple geometry of a long array of equally spaced scatterers. We shall refer to this as the 'large array approximation' (LAA). The essential idea is to assume that the array is sufficiently large to allow the ends to be treated separately, unless Rayleigh–Bloch (RB) surface waves are excited. These propagate without loss along the array, and can cause strong interactions between the ends. In particular, we will show how such interactions can lead to powerful forces being exerted on central elements of the array [2], and give a qualitative explanation of this effect. For simplicity, we will consider scattering of a plane wave by an array of cylinders parallel to the direction of propagation (head on incidence).

2 Notation

Consider a periodic array of bottom mounted vertical circular cylinders of radius a standing in a fluid of constant depth h. The problem is scaled so that the axis of cylinder p is located at the point $(p, 0)$ in the (x, y) plane, where $p = 0, 1, \ldots, P$, see Fig. 1. The plane wave

$$\phi^{\mathrm{i}} = \mathrm{Re}[\mathrm{e}^{\mathrm{i}kx}\mathrm{e}^{-\mathrm{i}\omega t}]\cosh[k(z + h)] \quad (1)$$

is incident upon the array. The depth and time dependence of all fields is identical to (1); henceforth we omit the factors $\mathrm{e}^{-\mathrm{i}\omega t}$ and $\cosh[k(z + h)]$, and also the symbol Re. We are left with a two dimensional scattering problem in which all fields $\phi(x, y)$ satisfy the Helmholtz equation $(\nabla^2 + k^2)\phi = 0$. Introducing shifted sets of polar co-ordinates (r_p, θ_p) with the origin positioned at the point $(p, 0)$, the boundary condition for the

total field may be expressed as $\partial\phi^{\mathrm{t}}/\partial r_p = 0$ on $r_p = a$.

In order to construct the LAA, we require the solutions to several canonical problems, in which the row of scatterers extends to infinity in one or more directions. Therefore we introduce the term '$\{p_0, p_1\}$ *array*' to refer to the array consisting of scatterers centred at $p = p_0, \ldots, p_1$. In general, the field scattered by such an array may be written in the form

$$\phi^{\mathrm{s}} = \sum_{p=p_0}^{p_1} \sum_{m=-\infty}^{\infty} \mathcal{U}_m^p Z_m \, \mathrm{H}_m^{(1)}(kr_p)\mathrm{e}^{\mathrm{i}m\theta_p}, \quad (2)$$

and the coefficients $\mathcal{U}_m^p$ satisfy the linear system

$$\mathcal{U}_m^p + \sum_{n=-\infty}^{\infty} Z_n \sum_{\substack{j=p_0 \\ \neq p}}^{p_1} \mathcal{U}_n^j X_{n-m}^{jp} \, \mathrm{H}_{n-m}^{(1)}(k|j - p|)$$
$$= \mathcal{R}_m^p. \quad (3)$$

Here $p = p_0, \ldots, p_1$, $m \in \mathbb{Z}$, $X_n^{jp} = 1$ if $p > j$ and $X_n^{jp} = (-1)^n$ if $p < j$. Also, $Z_m = \mathrm{J}_m'(ka)/\mathrm{H}_m^{(1)\prime}(ka)$. The quantity $\mathcal{R}_m^p$ on the right-hand side of (3) is determined by the incident field; for the plane wave (1) we have

$$\mathcal{R}_m^p = -\mathrm{e}^{\mathrm{i}pk}\mathrm{i}^m. \quad (4)$$

The order summations appearing in (2) and (3) (i.e. those over over m and n) converge exponentially and only a few terms are required to achieve a high degree of accuracy. However, if the array is large, so that $p_1 \gg p_0$, then directly solving (3) becomes computationally expensive. Since the incident field propagates parallel to the array, the problem is symmetric about $y = 0$, and this leads to the simplification $\mathcal{U}_m^p = (-1)^m\mathcal{U}_{-m}^p$. We write equations in such a way that the order summations range over all of $\mathbb{Z}$, since this is the most concise presentation. Symmetry is exploited to expedite numerical calculations, however.

3 Rayleigh–Bloch waves

At low frequencies, the $\{-\infty, \infty\}$ array can support RB surface waves. These propagate without loss along the array, and correspond to homogeneous solutions of (3). We therefore set $\mathcal{R}_m^p = 0$,
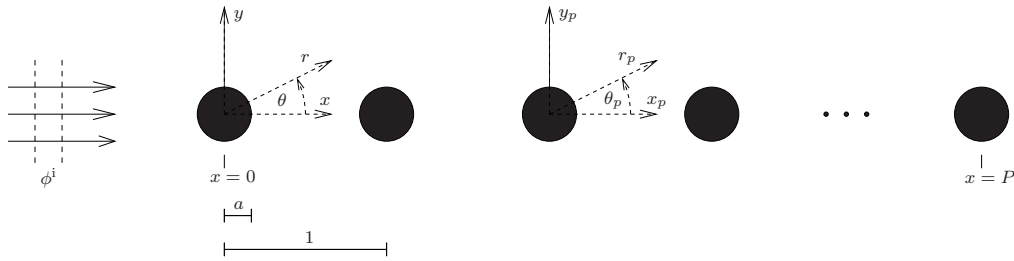
Fig. 1: Schematic diagram of the array.

for all $m, p \in \mathbb{Z}$, write

$$\mathcal{U}_m^p = \tilde{B}_m \mathrm{e}^{\mathrm{i}p\tilde{\beta}}, \qquad (5)$$

and seek values of $\tilde{\beta}$ for which (3) possesses a nontrivial solution. These can be determined using the method in [3], as can the nontrivial solution itself, which we scale so that $\sum_{m=-\infty}^{\infty} |\tilde{B}_m Z_m|^2 = 1$. Note that (5) represents a right-propagating mode; its left-propagating counterpart is obtained by replacing $\tilde{\beta}$ and $\tilde{B}_m$ with $-\tilde{\beta}$ and $(-1)^m \tilde{B}_m$, respectively. Given the evident 2π periodicity in (5), we may restrict attention to the range $\tilde{\beta} \in [0, \pi]$. For any given scatterer size $a \in (0, 0.5)$, RB waves that are symmetric about $y = 0$ exist at a range frequencies satisfying $0 < k < k_{\max} < \pi$. The value of the cut-off must be determined numerically; a plot of $k_{\max}$ against a is given in [4]. Numerical results will be presented here for $a = 0.25$ (as in [2]), in which case we have the approximate value $k_{\max} = 2.7826$. At the cut-off value, $\tilde{\beta} = \pi$ for all scatterer sizes, so that the RB wave ceases to propagate and takes the form of a standing mode. The fact that $\tilde{\beta} = \pi$ causes the system of equations for $\tilde{B}_m$ given in [3] to decouple into two subsystems, one each for the odd and even modes. In general, these two subsystems cannot both possess nontrivial solutions, and numerical results confirm that, when $k = k_{\max}$, $\tilde{B}_{2m} = 0$ for all m.

The canonical problem of the $\{0, \infty\}$ array under excitation of a left-propagating Raleigh–Bloch wave incident from the far field has not been previously considered. We consider an incident wave with unit amplitude, so that the total field for this problem can be written as

$$\phi^{\mathrm{t}} = \sum_{n=-\infty}^{\infty} Z_n \sum_{j=0}^{\infty} \left[(-1)^n \tilde{B}_n \mathrm{e}^{-\mathrm{i}j\tilde{\beta}} + Q_n^p \right]$$
$$\times \mathrm{H}_n^{(1)}(kr_j) \mathrm{e}^{\mathrm{i}n\theta_j}, \quad (6)$$

where, in terms of (3), $\mathcal{U}_m^p = Q_m^p$, i.e. Q_m^p represents the scattered response. The appropriate

form for $\mathcal{R}_m^p$ is obtained by taking the known term to the right-hand side, and exploiting the fact that the RB wave is a homogeneous solution to the $\{-\infty, \infty\}$ problem. We find that

$$\mathcal{R}_m^p = \mathrm{e}^{-\mathrm{i}p\tilde{\beta}} \sum_{n=-\infty}^{\infty} (-1)^n Z_n \tilde{B}_n \sum_{j=1+p}^{\infty} \mathrm{e}^{\mathrm{i}j\tilde{\beta}} \mathrm{H}_{n-m}^{(1)}(kj).$$
$$(7)$$

Now each coefficient Q_m^p includes a contribution from a right-propagating RB wave generated by reflection, therefore we write

$$Q_m^p = \rho \mathrm{e}^{\mathrm{i}p\tilde{\beta}} \tilde{B}_m + T_m^p, \qquad (8)$$

where $T_m^p \to 0$ as $p \to \infty$. The parameter ρ is the end reflection coefficient.

This problem can be trivially solved by inspection in the case where $k = k_{\max}$, when there is no distinction between the left- and right-propagating RB waves. Thus, if we take $\rho = 1$ and $T_m^p = 0$, then (3) is satisfied, since $\tilde{B}_{2m} = 0$ for all m. At other frequencies, the value of ρ and the coefficients T_m^p can be calculated numerically using the filtering methods developed in [4]. For all scatterer sizes, the magnitude of ρ remains small until k approaches $k_{\max}$, after which the real part increases sharply toward the limiting value 1.

We can obtain the leading order behaviour of the far field on the array (i.e. for $|y| < a$ and $x \to \infty$) in modal form by using an integral representation for $\mathrm{H}_n^{(1)}(kr) \mathrm{e}^{\mathrm{i}n\theta}$ [5]. A straightforward procedure shows that, in the limit $x \to \infty$,

$$\phi^{\mathrm{s}} \sim \sum_{j=-\infty}^{\infty} \tilde{A}_j \mathrm{e}^{\mathrm{i}ky\sin\tilde{\psi}_j} \left(\rho \mathrm{e}^{\mathrm{i}kx\cos\tilde{\psi}_j} + \mathrm{e}^{-\mathrm{i}kx\cos\tilde{\psi}_j} \right), (9)$$

which is valid for $y > 0$. Here, $k\cos\tilde{\psi}_j = \tilde{\beta} + 2j\pi$, $\sin\tilde{\psi}_j$ is positive real or positive imaginary, and

$$\tilde{A}_j = \frac{2}{k\sin\tilde{\psi}_j} \sum_{n=-\infty}^{\infty} (-\mathrm{i})^n \tilde{B}_n Z_n \mathrm{e}^{\mathrm{i}n\tilde{\psi}_j}. \qquad (10)$$

Equivalent results for $y < 0$ can be deduced by symmetry, but the modal form is not valid on $y = 0$. To an observer positioned in this region
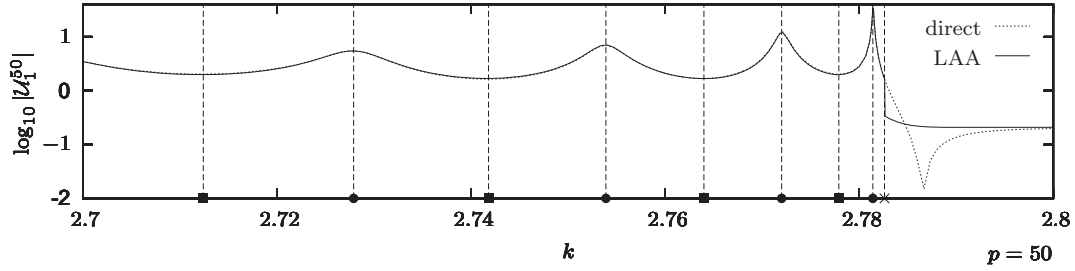
Fig. 2: Force on cylinder 50 of a 101 scatterer array, with $a = 0.25$ and varying k using the direct method and the LAA. Legend: $\times$ cut-off for symmetric RB modes, $\bullet$ ($\blacksquare$): peak (minimum) predicted by (15) and (16).

of the far field the array end appears to act as if there is a *'wall'* located at $x = -1/2$, with reflection coefficient $\rho e^{-i\tilde{\beta}}$. It turns out that the imaginary part of this quantity is negligible relative to the real part (which is negative) when k is close to $k_{\max}$. This is the root cause of the connection between the near trapping effect discussed in §5 and trapped modes on an array in a channel [2, 3]. The approximation $\text{Im}[\rho e^{-i\tilde{\beta}}] = 0$ generally gives very good results, and becomes increasingly accurate at the scatterer size a is reduced.

4 The large array approximation

We now construct an approximation to the scattered field generated by the plane wave (1) incident upon the $\{0, P\}$ array, according to the LAA. Thus, we write $\mathcal{U}_m^p = F_m^p$, where

$$F_m^p = A_m^p + \mu^+ Q_m^p + \mu^- e^{iP\tilde{\beta}} Q_{-m}^{P-p}. \quad (11)$$

Here, the first term on the right-hand side is generated directly by the impact of the incident field on the array, whereas the last two terms represent effects due to the repeated reflection of the RB waves. Thus, the coefficient A_m^p is obtained by considering scattering of the plane wave (1) by the $\{0, \infty\}$ array. Results in [4] show that

$$A_m^p = \alpha e^{ip\tilde{\beta}} \tilde{B}_m + C_m^p, \quad (12)$$

i.e. A_m^p includes a contribution due to a right-propagating RB wave with a (complex) amplitude coefficient α, and a contribution denoted C_m^p which decays as $p \to \infty$. The value of α depends upon the frequency and the scatterer size, and may be determined numerically (along with the coefficients C_m^p) using the double filtering method developed in [4].

Now the coefficient Q_m^p represents the response to a left-propagating RB wave of unit amplitude incident on the left end. If we consider the $\{-\infty, P\}$ array under excitation by a right-propagating RB wave of unit amplitude, we find

that the coefficients representing the scattered response are given by $\mathcal{U}_m^p = e^{iP\tilde{\beta}} Q_{-m}^{P-p}$. In view of this, the parameters μ^+ and μ^- are equal to the total amplitude of the left- and right-propagating RB waves, respectively, hence

$$\mu^+ = \rho e^{2iP\tilde{\beta}} \mu^-; \qquad \mu^- = \alpha + \rho \mu^+. \quad (13)$$

Solving these equations leads to

$$\mu^+ = \frac{\rho \alpha e^{2iP\tilde{\beta}}}{1 - \rho^2 e^{2iP\tilde{\beta}}}; \quad \mu^- = \frac{\alpha}{1 - \rho^2 e^{2iP\tilde{\beta}}}. \quad (14)$$

The amplitudes of the left- and right-propagating RB waves on the finite array are thus determined in terms of α and ρ, which are known from the solutions to the canonical problems. Note that the right-hand side of (11) remains finite as $\tilde{\beta} \to \pi$ (so that $\rho \to 1$), since both T_m^p and $\tilde{B}_{2m}$ vanish in this limit.

5 Near trapping

The modulus of the coefficient $\mathcal{U}_1^p$ represents the force in the x direction exerted by the wave field on element p of the array, normalised using the force exerted by a plane wave of unit amplitude on a scatterer in isolation. Strong forces have previously been observed at the centre of long arrays at certain discrete frequencies when k is close to the cut-off value $k_{\max}$; this effect is known as 'near trapping'. Part of the reason for this effect is simply the large value of the end reflection coefficient, ρ. Furthermore, at such frequencies, the phase of the RB wave is unaffected by traversing the array twice, and undergoing two reflections, that is the quantity $\rho^2 e^{2iP\tilde{\beta}}$ is positive real. Consequently, the left- and right-propagating RB modes are in phase with their respective multiple reflections, leading to constructive interference. Given that $\text{Im}[\rho e^{-i\beta}] \approx 0$, the frequencies correspond to values of $\tilde{\beta}$ satisfying

$$\tilde{\beta} \approx [1 - q/(P+1)]\pi, \quad q = 1, 2, \ldots, P. \quad (15)$$

Increasing P allows $\tilde{\beta}$ to take a value closer to π (thus increasing $|\rho|$), therefore near trapping is more prevalent on larger arrays.

195
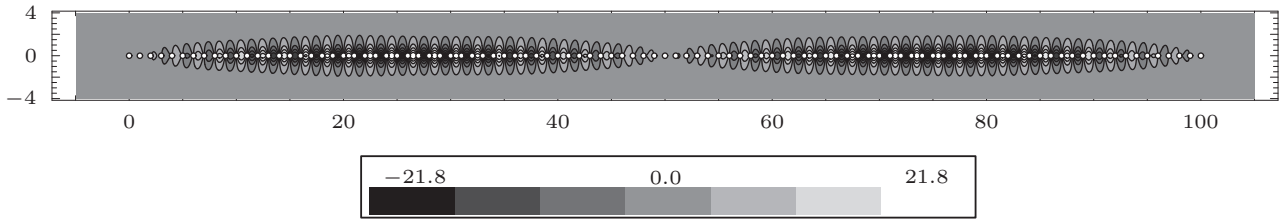
Fig. 3: Contour plot showing $\mathrm{Re}[\phi^{\mathrm{t}}]$ for a 101 scatterer array, with $a = 0.25$ and $k = 2.7778$.

Fig. 2 shows logarithmic plots of the horizontal force on the center cylinder of a 101 scatterer array, with $a = 0.25$ and varying k. The coefficients C_m^p and T_m^p were computed numerically for $p \leq 50$. For $p > 50$, the leading order asymptotic form is used; see [4]. Similar results have been obtained for larger arrays, without increasing the accuracy with which the canonical problems are solved. The only discrepancy between the LAA and the exact theory occurs when k is slightly larger than the cut-off value k_{max}^s. The most likely cause of this is that the RB modes, which have been omitted from the LAA for $k > k_{\mathrm{max}}^s$ are now evanescent in x, but can still cause interactions between the ends when $\mathrm{Im}[\tilde{\beta}]$ is small. The locations at which peaks and troughs occur in the force can be predicted using equations (8), (11) and (14). Thus, the left- and right-propagating RB waves are in phase with eachother when p is chosen so that the quantity $1 - \rho \mathrm{e}^{2\mathrm{i}(P-p)\tilde{\beta}}$ is maximised, and out of phase when it is minimised. Retaining the approximation that $\rho \mathrm{e}^{-\mathrm{i}\beta}$ is negative real, and applying (15), we find that

$$1 - \rho \mathrm{e}^{2\mathrm{i}(P-p)\tilde{\beta}} \approx 1 - |\rho| \mathrm{e}^{\mathrm{i}q\pi(2p+1)/(P+1)}. \quad (16)$$

If, as is the case here, we are concerned with the force at the centre of the array then, since $p = P/2$, odd and even values for q cause the waves to be in and out of phase with eachother, respectively. The corresponding frequencies are shown in Fig. 2; the agreement is excellent.

Fig. 3 shows a contour plot for $k = 2.7778$ on a 101 scatterer array, with $a = 0.25$ as before. Note that this is a plot of the real part of the *total* field, but the incident wave is not visible due to the strength of the near trapping effect. This wavenumber corresponds to taking $q = 2$ in (15), and is the right-most point marked with a '■' in Fig. 2. Consequently, (16) predicts that elements close to $p = 25$ and $p = 75$ are subject to the greatest force, whereas the force on the central elements is small.

6   Concluding remarks

We have developed a new method for investigating scattering by long arrays of circular cylinders, based on the use of solutions to certain canonical problems. Whilst this includes a numerical element, the required computation time is largely determined by the speed at which the canonical solutions can be calculated, and is barely affected by increasing the array size. It therefore offers considerable reductions in computation time over the direct method. Furthermore, the LAA offers significantly improved insight into scattering by large arrays. In particular, it accurately captures the effect of near trapping, where large forces are exerted on certain elements of the array, and facilitates predictions of the frequencies at which this can occur. In this paper, we have considered only head-on incidence upon a linear array of cylinders, however the method is not restricted to this case. It can also be used for arrays consisting of multiple rows, and different shaped scatterers, provided that the relevant canonical problems can be solved. The case of oblique incidence is a simple extension requiring only that excitation of both ends of the array by the incident field is taken into account. Numerical results for this case will be shown at the workshop.

References

[1] C. M. Linton and P. McIver. *Handbook of Mathematical Techniques for Wave/Structure Interactions*. Chapman & Hall/CRC, Boca Raton, 2001.

[2] H. D. Maniar and J. N. Newman. Wave diffraction by a long array of cylinders. *J. Fluid Mech.*, 339:309–330, 1997.

[3] D. V. Evans and R. Porter. Trapping and near-trapping by arrays of cylinders in waves. *J. Engng. Math.*, 35:149–179, 1999.

[4] C. M. Linton, R. Porter, and I. Thompson. Scattering by a semi-infinite periodic array and the excitation of surface waves.[1]

[5] P. A. Martin. *Multiple Scattering. Interaction of Time-Harmonic Waves with N Obstacles*. Cambridge University Press, 2006.

[1]Preprint available from `http://www.lboro.ac.uk/departments/ma/research/preprints/`